Neuron, Vol. 14, 209–220, April 11, 2002, Copyright ©2002 by Cell Press

Signaling Microdomains Define the Specificity of Receptor-Mediated $InsP_3$ Pathways in Neurons

Patrick Delmas,[1,2,3] Nicolas Wanaverbecq,[1] Fe C. Abogadie,[1] Mohini Mistry,[1] and David A. Brown[1]
[1]Wellcome Laboratory for Molecular Pharmacology
Department of Pharmacology
University College London
Gower Street
London, WC1E 6BT
United Kingdom
[2]Intégration des Informations Sensorielles, CNRS
31 Chemin Joseph Aiguier
13402 Marseille cedex 20
France

Summary

M_1 muscarinic (M_1AChRs) and B_2 bradykinin (B_2Rs) receptors are two PLCβ-coupled receptors that mobilize Ca^{2+} in nonexcitable cells. In many neurons, however, B_2Rs but not M_1AChRs mobilize intracellular Ca^{2+}. We have studied the membrane organization and dynamics underlying this coupling specificity by using Trp channels as biosensors for real-time detection of PLCβ products. We found that, in sympathetic neurons, although both receptors rapidly produced DAG and $InsP_3$ as messengers, only $InsP_3$ formed by B_2Rs has the ability to activate IP_3Rs. This exclusive coupling results from spatially restricted complexes linking B_2Rs to IP_3Rs, a missing partnership for M_1AChRs. These complexes allow fast and localized rises of $InsP_3$, necessary to activate the low-affinity neuronal IP_3R. Thus, these signaling microdomains are of critical importance for the induction of selective responses, discriminating proinflammatory information associated with B_2Rs from cholinergic neurotransmission.

Introduction

Coordination of cellular functions resides in the ability of a cell to convert extracellular stimuli into appropriate cellular responses. These cellular responses are dictated by the nature of the signal transduction pathway initiated by the receptor. However, in any individual cell, the number of signaling proteins appears limited, and often these proteins are molecular targets for multiple plasma membrane receptors. A persistent dilemma therefore is how receptors that are coupled to identical transducing proteins and second messenger systems can produce different output signals. One possibility is that specificity results from differences in spatial organization and dynamics in the receptor-transduction systems. Structural mechanisms for the spatial organization of some G protein-coupled receptors (GPCRs) are known (e.g., *Drosophila* photoreceptors and metabotropic glutamate receptors) (Hardie and Raghu, 2001; Fagni et al., 2000; Xiao et al., 2000), but there is no comparable information about the differential organization and dynamics of GPCRs activating the same effector system within a single neuron.

Here, we explore the question of how different neurotransmitter receptors that utilize one common pathway—the phospholipase C (PLC) pathway—can induce different responses in the same neuron. The PLC pathway provides a ubiquitous mode of transduction in eukaryotic cells that regulates fundamendal cell functions as diverse as gene expression, exocytosis, neuronal signaling, cell growth, and differentiation and is the focal point for signal transduction triggered by G protein-coupled receptors and tyrosine kinase receptors (Berridge, 1993, 1998). Active PLC catalyses the breakdown of phosphatidylinositol biphosphate into the second messengers diacylglycerol (DAG) and inositol-1,4,5-triphosphate ($InsP_3$). DAG is the physiological activator of the different members of the protein kinase C family, while $InsP_3$ mobilizes Ca^{2+} from internal IP_3R-stores.

M_1 muscarinic (M_1AChR) and B_2 bradykinin (B_2R) receptors are two G protein-coupled receptors that activate PLC. M_1AChRs play a key role in regulating neuronal excitability (Caulfield, 1993; Brown et al., 1997; Hamilton et al., 1997), whereas B_2Rs mediate inflammation and hyperalgesia (Dray and Perkins, 1993; Dray, 1997). In nonexcitable cells, stimulation of either of these two receptors leads to PLC-mediated production of $InsP_3$, which triggers release of Ca^{2+} through endoplasmic reticulum-associated $InsP_3$ receptors (IP_3R) (Felder, 1995; Lee and Rhee, 1995). Surprisingly, however, in neurons, M_1AChRs appear to be relatively weak mobilizers of intracellular Ca^{2+}. A typical example is found in rat sympathetic neurons, which express both M_1AChRs and B_2Rs (Marrion et al., 1989; Bernheim et al., 1992; Jones et al., 1995; Hamilton et al., 1997). While stimulation of either receptor can activate PLC sufficiently to increase the formation of $InsP_3$ (del Río et al., 1999; Bofill-Cardona et al., 2000) and DAG, with consequent mobilization of protein kinase C (Marsh et al., 1995), only B_2Rs produce a significant rise in intracellular Ca^{2+} (Cruzblanca et al., 1998; del Río et al., 1999). This implies that only the B_2R efficiently couples to the endoplasmic IP_3R, and raises the question, what membrane organization of receptors and transducing molecules might underly this differential coupling?

In the present study, we have tried to answer this question by dynamically tracing receptor-mediated PLC signals in individual neurons. We have developed the use of exogenously expressed mammalian homologs of the *Drosophila* transient receptor potential (Trp) proteins as biosensors for PLC signaling. Trp homologs form cation channels (TrpC) that are activated by signaling events downstream from receptor activation and PLC stimulation (Zhu et al., 1996; Harteneck et al., 2000; Clapham et al., 2001). In particular, we used mouse TrpC6 and human TrpC1, which are activated by DAG (Hofmann et al., 1999) and via IP_3Rs (Lockwich et al., 2000; Rosado and Sage, 2000), respectively. The activity of these channels was found to be a high-fidelity indicator

[3]Correspondence: delmas@irlnb.cnrs-mrs.fr

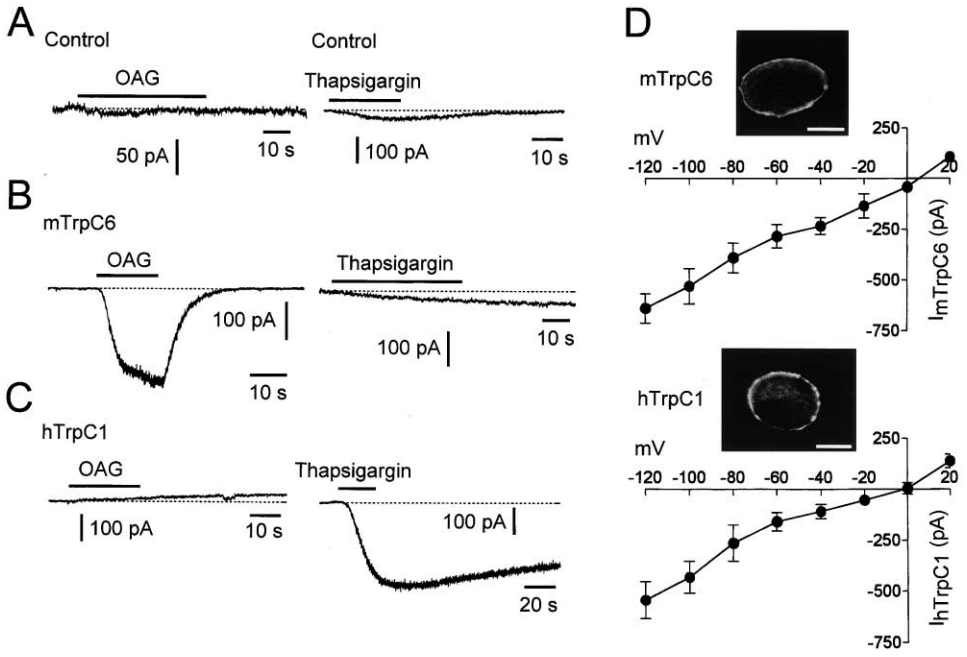

Figure 1. Mechanism of Activation of hTrpC1 and mTrpC6 in SCG Neurons

(A–C) Effects of 1-oleoyl-2-acetyl-glycerol, OAG (50 μM), and thapsigargin (500 nM) recorded in control neurons (A) and in neurons expressing either mTrpC6 (B) or hTrpC1 (C). Cells were voltage clamped at −70 mV using the perforated patch method.

(D) mTrpC6 and hTrpC1 I-V relationships. TrpC I-V relationships are difference-currents obtained by subtracting I-V curves before and after application of OAG (mTrpC6 current) or thapsigargin (hTrpC1 current). Points are mean ± SEM (n = 5–7). Insets, confocal sections showing plasma membrane expression of myc-tagged mTrpC6 and myc-tagged hTrpC1. Scale bars, 10 μm.

of PLC stimulation when expressed in neurons, providing a real-time detection device for submembrane production of DAG and $InsP_3$. These experiments were paralleled by testing the ability of M_1AChRs and B_2Rs to translocate GFP-tagged DAG- or Ca^{2+}-sensing domains of PKCγ. Using these approaches in combination with patch-clamp recording of macroscopic and microscopic membrane domains, we show that although both M_1AChR and B_2R are indeed robust activators of PLCβ, only $InsP_3$ produced by B_2R had the ability to activate reticular IP_3Rs. This peculiarity results from a membrane arrangement that links IP_3Rs to B_2Rs, but not M_1AChRs, allowing $InsP_3$ to be produced at the required concentration and the precise location inside the cell. Thus, membrane-transducing microdomains play a key role in spatio-temporal coding of $InsP_3$ signals, enabling the cell to discriminate between identical signaling pathways that are triggered by different membrane receptors.

Results

Trp Channels as Biosensors for Detecting Submembrane PLC Products in Neurons

We first determined the properties of activation of Trp channels expressed in superior cervical ganglion (SCG) neurons. Nuclei of SCG neurons were microinjected with cDNA constructs encoding hTrpC1, hTrpC3, and mTrpC6 and perforated-patch somatic recordings were made 12–24 hr later. Expression of these TrpC minigenes in SCG neurons did not produce constitutive activity.

In cells expressing mTrpC6, 1-oleoyl-2-acetyl-*sn*-glycerol (OAG, 50 μM) produced inward currents that were absent in control cells (Figures 1A and 1B). Mouse TrpC6 inward currents were not activated by activators of PKC (pdBU 500 nM, n = 5) or by thapsigargin (TG), an inhibitor of endoplasmic reticulum Ca^{2+}-ATPase (Figure 1B, n = 6). OAG-induced mTrpC6 currents displayed properties of nonselective cation currents with an apparent reversal potential of +4 ± 3 mV (Figure 1D, n = 7). These currents were blocked by 90%–97% by 100 μM La^{3+}, as expected for this family of Trp channels (Boulay et al., 1997).

Cytoplasmic injection of $InsP_3$ at a final intracellular concentration of ~15 μM (see Experimental Procedures) activated hTrpC1 but not mTrpC6 (Figure 3; n = 4–6). Lower $[InsP_3]_i$ were largely ineffective in stimulating hTrpC1. hTrpC1-expressing cells also responded to TG by large inward currents (Figure 1C) that reversed at −1 ± 4 mV (Figure 1D, n = 5) and were blocked by La^{3+}. Bath application of OAG had no effect on hTrpC1 (Figure 1C, n = 9), whereas hTrpC3 could be activated by either OAG (n = 6 of 7) or microinjection of $InsP_3$ ($[InsP_3]_i$ ~15 μM, n = 3 of 4) (data not shown).

Taken together, these data indicate that mTrpC6 expressed in SCG neurons is activated by OAG, independently of PKC, whereas hTrpC1 is activated via an $InsP_3$-dependent mechanism. This accords with previous studies in cell lines showing gating of TrpC6 by DAG analogs and activation of TrpC1 by $InsP_3$ or TG (Boulay et al., 1997; Hofmann et al., 1999; Rosado and Sage, 2000). In the subsequent experiments, we therefore used mTrpC6 and hTrpC1 as real-time sensors of the

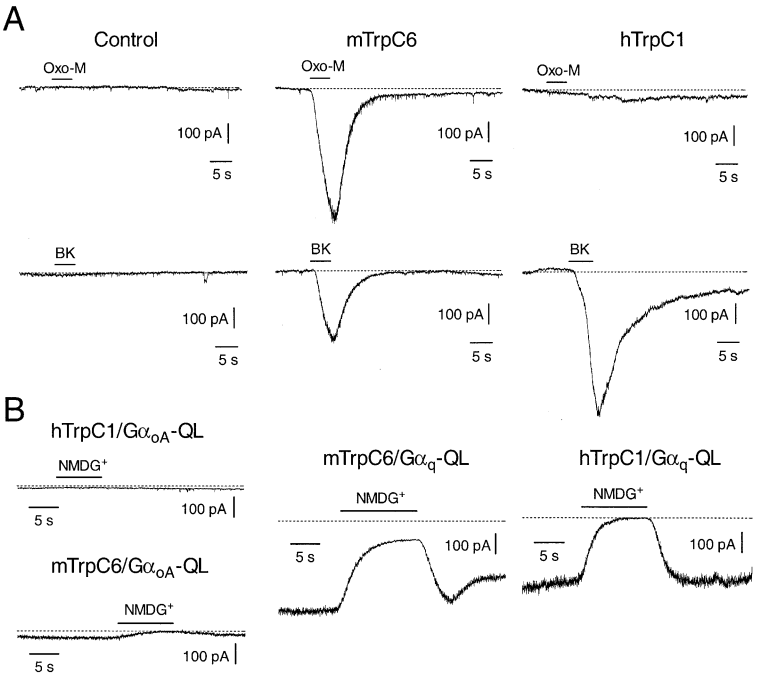

Figure 2. Differential Activation of TrpC by M_1AChRs and B_2Rs

(A) Shown are inward currents induced by oxotremorine-M (Oxo-M, 5 μM, top traces) and bradykinin (BK, 100 nM, bottom traces) in control cells and in cells expressing either mTrpC6 or hTrpC1 (as indicated). Holding potential, −80 mV.

(B) Tonic activation of mTrpC6 and hTrpC1 cation currents in neurons coexpressing GTPase-deficient forms of $G\alpha_q$ but not $G\alpha_{oA}$ subunits ($G\alpha_q$-QL and $G\alpha_{oA}$-QL, respectively). Horizontal bars indicate isoosmotic substitution of external Na^+ by N-methyl-D-glucosamine, $NMDG^+$. Holding potential, −70 mV.

PLCβ products DAG and $InsP_3$, respectively. Human TrpC3 was not used further as at least two distinct routes (DAG and $InsP_3$) appeared to activate this channel in our system (in agreement with Ma et al., 2000).

We confirmed the plasma membrane distribution of TrpC in sympathetic neurons by expressing cDNA constructs encoding mTrpC6 and hTrpC1 C-terminally fused to myc-tag. Both fusion proteins formed functional channels with properties indistinguishable from the channels lacking the c-*myc* tags (n = 4–5). mTrpC6 and hTrpC1 were prominently targeted to the plasma membrane (insets in Figure 1D).

Different Ability of B_2R and M_1AChR to Activate Trp Channels

To trace receptor signals, we tested the ability of constitutively expressed B_2Rs and M_1AChRs to couple to TrpC. The concentration of agonists were chosen to be saturating (see below). In control neurons held at −70 mV, neither bradykinin (BK, 100 nM) nor the muscarinic agonist oxotremorine-M (Oxo-M, 5 μM) produced inward currents (Figure 2A). Reversible cation currents developed in response to both BK and Oxo-M in cells expressing mTrpC6 (Figure 2A and Table 1). By contrast, in neurons expressing hTrpC1, only BK was able to generate large inward currents while Oxo-M was ineffective (n = 11 of 11; Figure 2A). Stimulation of the $G_{i/o}$ protein-coupled α_2-adrenoceptor by norepinephrine had no effect in cells expressing either hTrpC1 or mTrpC6 (n = 4–6, data not shown). The EC_{50} value for activation of mTrpC6 by Oxo-M was 450 ± 35 nM (n = 5). Higher concentrations of Oxo-M (>10 μM) did not produce activation of hTrpC1. However, in some cases, rapid inward currents were observed with these high concentrations of Oxo-M. They were fully blocked by the nicotinic receptor antagonist, hexamethonium (100 μM), implying a contribution of nicotinic receptors. EC_{50} for activation of mTrpC6 and hTrpC1 by BK were 6 ± 3.5 nM (n = 5) and 12 ± 5 nM (n = 6), respectively.

Activation of TrpCs by Oxo-M and/or BK was resistant to overnight treatment with *pertussis* toxin (PTX), consistent with the coupling specificity of M_1AChR and B_2R to PTX-insensitive G proteins (Delmas et al., 1998b; Haley et al., 1998; Haley et al., 2000a). In order to identify further the G protein species involved, GTPase-deficient forms of G protein α subunits (GαQ-L) were expressed together with Trp channels. Tonic activation of TrpC currents was then detected as a standing inward current

Table 1. Receptor/G Protein Coupling to Trp Channels in SCG Neurons

Treatment	Oxo-M	BK	NE	G_qQL	$G_{11}QL$	$G_{oA}QL$	G_zQL	$G_{12}QL$
Current density[a] (pA/pF) Control	0–0.18	0–0.5	0–0.3	0–0.3	0–0.2	0–0.5	0–0.7	0–0.8
mTrpC6	13 ± 2[c]	6 ± 1[c]	0.1 ± 0.2	11.8 ± 3[c]	9 ± 2[c]	1.4 ± 0.7	0.3 ± 0.3	0.7 ± 0.3
hTrpC1	0.9 ± 0.4	17 ± 3[c]	0.5 ± 0.3	8.4 ± 2[c]	6 ± 2[c]	0.6 ± 0.2	0.2 ± 0.1	1.1 ± 0.4
hTrpC3	4.6 ± 2[b]	3.5 ± 1[b]	0.4 ± 0.2	5 ± 2[b]	NT	NT	0.4 ± 0.3	NT

Saturative concentrations were used: [Oxo-M] 5μM, [BK] 100 nM, and [NE] 1μM. NT, not tested.

[a] As estimated from the $NMDG^+$-sensitive inward current.

[b] $p < 0.05$ versus control (one-way ANOVA and Dunnest's multiple comparison test).

[c] $p < 0.01$ versus control. (one-way ANOVA and Dunnest's multiple comparison test.)

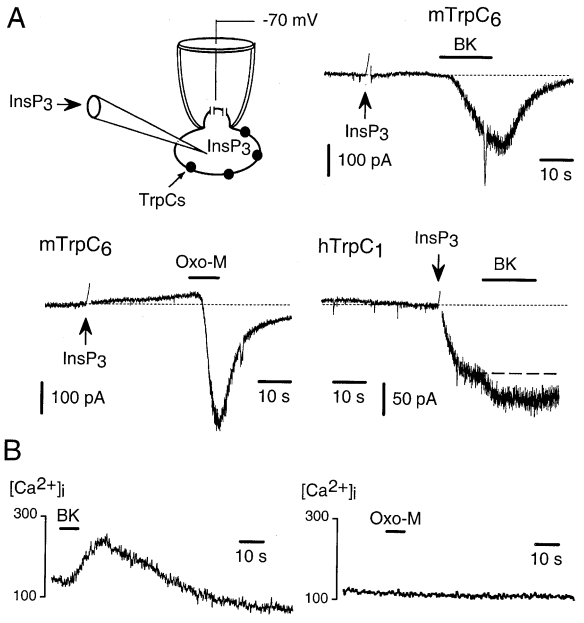

Figure 3. The B_2R, but Not the M_1AChR, Couples to hTrpC1 via IP_3R

(A) Top left panel, schematic diagram of intracellular microinjection of $InsP_3$ during perforated patch-clamp recording. Cytoplasmic microinjection of $InsP_3$ (0.5 pl at 100 μM, arrows) activated hTrpC1 but not mTrpC6. Note that $InsP_3$ occluded the activation of hTrpC1 by BK (100 nM) but not activation of mTrpC6.

(B) BK (100 nM) but not Oxo-M (5 μM) mobilized intracellular Ca^{2+} in control neurons. All cells were voltage clamped at −60 mV.

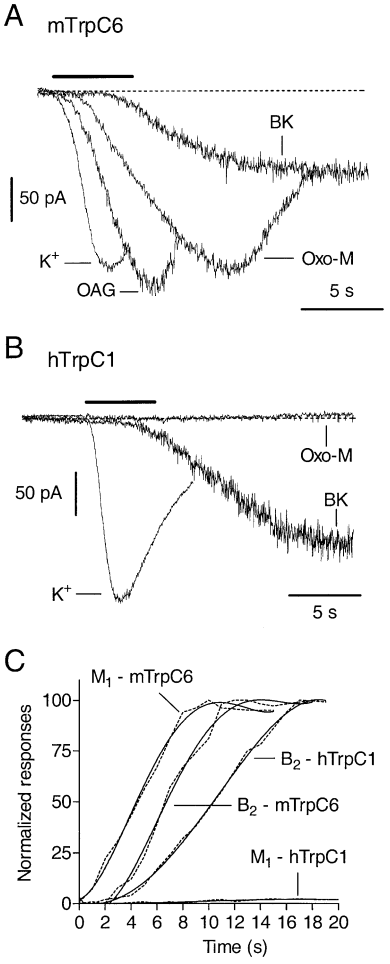

Figure 4. Kinetics of Receptor-Mediated Production of DAG and $InsP_3$ in Individual Neurons

Time course of activation of mTrpC6 (A) and hTrpC1 (B) in response to bath application of BK, Oxo-M, and/or OAG. Inward currents induced by a high external K^+ solution (40 mM) have been rescaled for comparison. Agonists have been applied for 5 s and high K^+ for 2 s. Same concentrations as in Figures 1 and 2.

(C) Rate of production of DAG and $InsP_3$ by M_1AChR and B_2R as detected with Trp channels. Dashed, broken lines are rising phases of the currents averaged from three to four cells, and smooth solid lines are polynomial fits to the data. T = 0 (s) indicates the onset of mTrpC6 activation by Oxo-M.

sensitive to either La^{3+} or external Na^+ substitution. Human TrpC1 and mTrpC6 currents (revealed by substituting N-methyl-D-glucosamine, NMDG, for external Na^+) were seen with $G\alpha_qQ$-L and $G\alpha_{11}Q$-L mutants but not with $G\alpha_{oA}Q$-L, $G\alpha_zQ$-L, and $G\alpha_{12}Q$-L mutants (Figure 2B and Table 1).

Both B_2R and M_1AChR Stimulate PLCβ, but Only B_2R Mobilizes IP_3R

Activation of hTrpC1 by BK and of mTrpC6 by Oxo-M were blocked by application of U73122 (10 μM for 10 min, n = 4–6), an inhibitor of PLC, but not by calphostin C (500 nM for 10 min, n = 3–5), a specific inhibitor of PKC. This is consistent with the involvement of PLCβ in the modulation of both hTrpC1 and mTrpC6. The stimulation of hTrpC1 by BK was blocked by the membrane-permeable inhibitors of IP_3R, xestospongin C (50 μM, n = 6) and diphenylboric acid 2-amino-ethyl ester (2APB, 80 μM, n = 5; see Figures 7 and 8). These agents had no significant effect on mTrpC6 currents activated by either BK or Oxo-M (paired t tests, $p > 0.1$, n = 5–6). Consistent with this, preactivation of hTrpC1 by cytosolic $InsP_3$ occluded by 91% (n = 6) further activation of hTrpC1 by BK (Figure 3A). Thus, although both M_1AChRs and B_2Rs stimulate PLCβ, activation of IP_3R-operated hTrpC1 was strictly restricted to B_2Rs. This preferential coupling was correlated with the ability of B_2Rs to mobilize Ca^{2+} from intracellular IP_3R-stores in both the somata (Figure 3B; see also Cruzblanca et al., 1998) and dendrites of control neurons. In contrast, Ca^{2+} mobilization was not detectable either in somata or dendrites in response to M_1AChR stimulation (Figure 3B; in agreement with Cruzblanca et al., 1998; del Río et al., 1999). Addition of the protein phosphatase inhibitors, okadaic acid (PP1/PP2A, 1 μM, n = 6), calyculin A (PP1, PP2A, 50 nM, n = 5), and FK506 (PP2B, 100 nM, n = 4) to the bath had no significant effect on the lack of coupling of M_1AChRs with either Ca^{2+} organelles or hTrpC1.

Kinetics of Receptor-Mediated Production of DAG and $InsP_3$ in Individual Neurons

We examined the kinetics of production of DAG and $InsP_3$ in response to B_2R and M_1AChR stimulation. In these experiments, a fast perfusion system was used and the responses to high external K^+ and OAG were taken as estimates for solution exchange and "direct" modulation, respectively (Figures 4A and 4B). When cor-

rection is made for the time course of solution exchange (Figure 4C), mTrpC6 currents developed with a similar rate of rise (10–12 ± 2% s^{-1}) in response to either Oxo-M or BK. However, responses to BK were consistently delayed by 2 ± 1 s (n = 7), perhaps indicating that binding of BK to B_2Rs is rate limiting (see also Jones et al., 1995). This later inference is substantiated by the faster activation of mTrpC6 by OAG (Figure 4A). BK activated hTrpC1 with a slower rising rate of 6.7 ± 2% s^{-1} (Figure 4C), probably reflecting additional downstream steps including the activation of IP_3Rs.

DAG- and Ca^{2+}-Sensing Domains of PKCγ Are Differentially Translocated by M_1AChR and B_2Rs

The above data indicate that both B_2Rs and M_1AChRs activate PLCβ, but only B_2Rs mobilize IP_3R-stores. We sought an alternative assay to verify this selective coupling, by testing the ability of B_2Rs and M_1AChRs to translocate DAG- and Ca^{2+}- binding domains of PKCγ ($C1_2$ and C2, respectively). A previous study in basophilic leukemia cells has shown that the translocation of $C1_2$ to the plasma membrane is induced by DAG, whereas the translocation of C2 depends on Ca^{2+} binding (Oancea and Meyer, 1998). cDNAs encoding GFP-tagged $C1_2$ and C2 domains of PKCγ were microinjected into the nuclei of neurons, and translocation was assessed 8–16 hr later in the absence of external Ca^{2+}. Figure 5 shows images of neurons expressing $C1_2$-GFP and C2-GFP under control conditions and after receptor stimulation. In the controls, $C1_2$-GFP and C2-GFP were seen in greatest density in the cytosol (Figure 5B). DAG-sensing $C1_2$ domain translocated to the plasma membrane in response to OAG application and to stimulation of both M_1AChRs and B_2Rs (n = 14 of 19 and n = 12 of 18, respectively). Other receptors such as the $G_{i/o}$-coupled α_2-adrenoceptor and somatostatin receptors were ineffective (n = 6–11). The Ca^{2+}-sensing C2 peptide translocated to the plasma membrane in response to TG and the Ca^{2+} ionophore, ionomycin (in the presence of 0.5 mM external Ca^{2+}). Addition of BK led to a marked translocation of C2-GFP to the plasma membrane (n = 11 of 17) (Figure 5B). This change in distribution can be clearly seen using a line scan analysis of the fluorescence across the cell (Figure 5C). BK-induced translocation was fully suppressed by preincubation of cells with xestospongin C (20 μM for 10 min; n = 6 of 6). In contrast, no plasma membrane translocation of C2-GFP was observed after Oxo-M addition (n = 17 of 17) (Figures 5B and 5C).

Cell Dependence of M_1AChR Coupling to IP_3R

We also tested the ability of M_1AChRs to activate IP_3R in nonneuronal cells and neuroblastoma hybrid cells. We used CHO cells and NG108-15 mouse neuroblastoma × rat glioma hybrid cells (clone BM-8) stably transfected with the human M_1 muscarinic receptor. NG108-15 cells also constitutively express B_2Rs (Fukuda et al., 1988). In these two cell lines, M_1AChR (as well as the B_2R, data not shown) activated transfected hTrpC1 (70%–85% of responsive cells). A representative experiment obtained in CHO cells is shown in Figure 6B. This property of the M_1AChR was associated with its ability to mobilize intracellular Ca^{2+} from IP_3R-stores in control

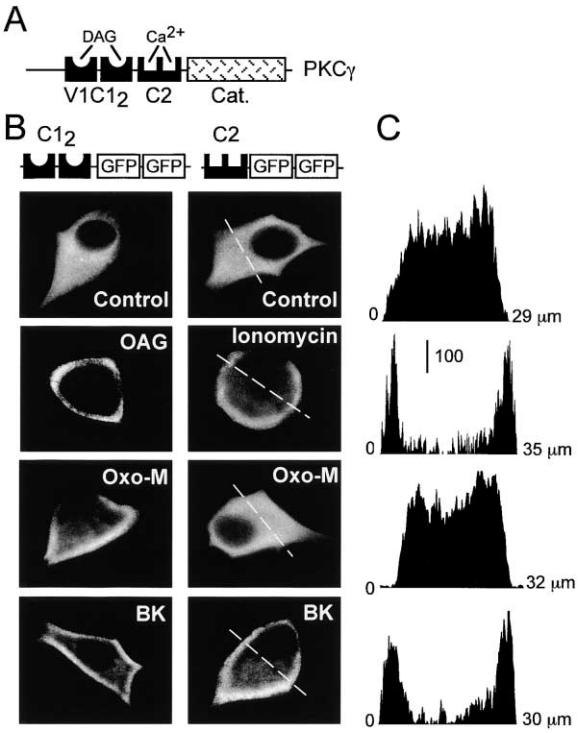

Figure 5. Receptor-Mediated Translocation of DAG- and Ca^{2+}-Sensing Domains of PKCγ

(A) Schematic representation illustrating DAG- and Ca^{2+}-binding domains of PKCγ.

(B) Distribution of $C1_2$-GFP (left panels) or C2-GFP (right panels) fusion proteins in neurons before and after addition of the drugs indicated (see Experimental Procedures for more details on drug application).

(C) Line scan profiles of the fluorescence intensity for the C2-GFP-expressing cells shown in (B).

cells (Figure 6A; see also Robbins et al., 1993). M_1AChR stimulation also translocated the initially cytosolic C2-GFP fusion protein to the plasma membrane in CHO cells (Figure 6C, n = 14 of 16). All these responses were abolished by 10 min pretreatment with xestospongin C (n = 3–8).

In clear contrast to primary sympathetic neurons, microinjection of low concentrations of $InsP_3$ were able to activate hTrpC1 in both CHO and NG108-15 cells. $[InsP_3]_i$ of less than 1 μM resulted in consistent activation of hTrpC1 in NG108-15 cells (n = 6 of 7), whereas even lower concentrations (~250 nM) were sufficient in CHO cells (n = 2, due to difficulties in impaling these flat cells).

Block of Calmodulin Reveals Remote Production of $InsP_3$ by M_1AChR

Calmodulin (CaM) has been shown to be responsible for the Ca^{2+}-dependent inactivation of type-1 IP_3R (Michikawa et al., 1999). We therefore tested whether CaM can act as a negative feedback regulator of receptor-mediated activation of IP_3Rs in our neuronal system. To do this we used mutants of rat CaM (CaM_{1-4}) in which the aspartate residue found in the first position of each of the four Ca^{2+} binding E-F hand motifs have been

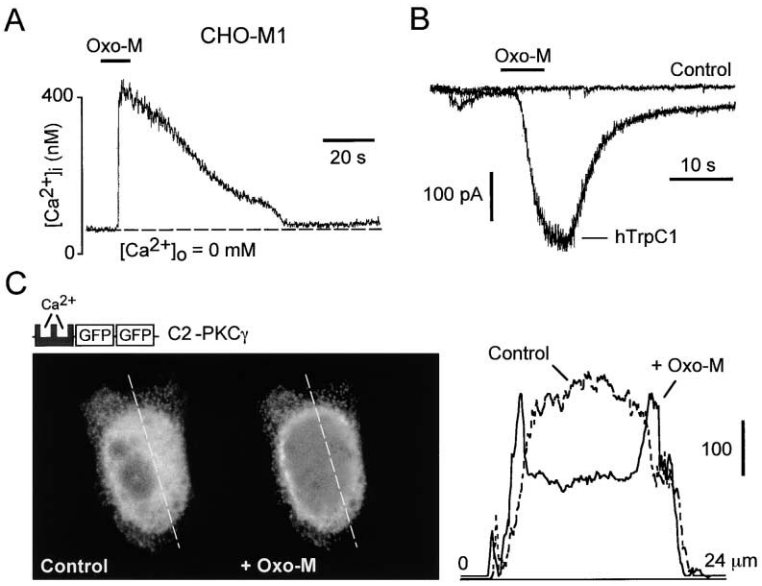

Figure 6. Activation of hTrpC1 and Mobilization of Ca^{2+} by M_1AChRs in CHO Cells

(A and B) Oxo-M (5 μM) mobilizes $[Ca^{2+}]_i$ (A) and activates hTrpC1 (B) in CHO cells stably transfected with M_1AChR. Holding potential, −70 mV.

(C) Oxo-M addition leads to the plasma membrane translocation of the Ca^{2+}-sensing C2-GFP in a living CHO cell. Right panel, line scan of the fluorescence intensity across the cell before and after Oxo-M addition.

mutated to an alanine. Such mutations reduced or abolished Ca^{2+} binding (Xia et al., 1998). Mutant CaMs were expressed in neurons and activation of hTrpC1 by B_2Rs or M_1AChRs was examined (Figure 7). In cells expressing CaM_{1-4}, BK produced hTrpC1 currents qualitatively similar to those recorded in control cells or cells expressing wt CaM. However, the peak amplitude of these currents was slightly increased (by 0.95 ± 0.2 pA/pF, n = 7), and their deactivation rate after removal of agonist was markedly slowed (Figure 7A). The slow deactivation and the slight increase of hTrpC1 currents resulted from the reduced inactivation of IP_3Rs in the presence of CaM_{1-4}, as evidenced by the effects of 2-APB (Figure 7A). Interestingly, in the presence of CaM_{1-4}, M_1AChR stimulation was now also capable of activating hTrpC1 (n = 6 of 10, Figure 7B). Activation of hTrpC1 by M_1AChRs however remained weak and 4- to 7-fold slower in onset than BK responses, suggesting that the M_1AChRs were rather remote from the IP_3R-stores, leading to a diffusional delay in the effect of $InsP_3$. As in control cells, Oxo-M had no effect in cells expressing wt CaM.

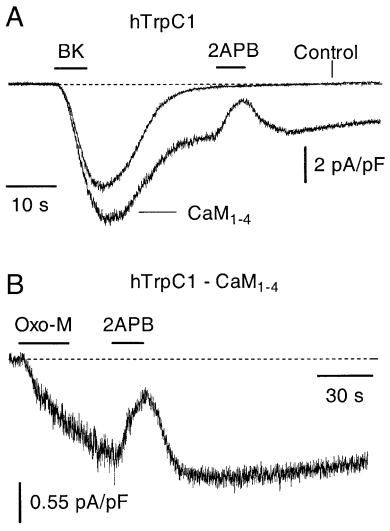

Figure 7. IP_3R Activation by M_1AChRs Is Unmasked by Dominant-Negative Calmodulin

(A) hTrpC1 currents evoked by BK (100 nM) in neurons expressing hTrpC1 alone (control trace) or coexpressing hTrpC1 and dominant-negative CaM_{1-4}. Note the slow deactivation of the hTrpC1 current following agonist removal in the presence of CaM_{1-4}. Currents were normalized to cell capacitance for comparison.

(B) Slow developing hTrpC1 current in response to Oxo-M (5 μM) in a neuron expressing dominant-negative CaM_{1-4}. Note the different scale bars in (A) and (B). 2 APB, 80 μM.

We also tested the effects of Oxo-M (5 μM) before and after treatment with the calmodulin inhibitor, calmidazolium (1 μM for > 5 min), in neurons expressing hTrpC1. Oxo-M activated a modest TrpC1 current (−35 ± 5 pA) in the presence of calmidazolium in five out of nine cells tested, whereas no current (−2 ± 1.2 pA) could be observed before treatment (data not shown). This current could be fully blocked by xestospongin-C treatment (20 μM, n = 4) and by bath application of La^{3+} (100 μM, n = 3). In control cells (uninjected) and cells expressing mTrpC6 (n = 5 and 4, respectively), the combination of Oxo-M and calmidazolium had no effect.

Actin Cytoskeleton Is Essential for B_2R Coupling to IP_3R

The actin cytoskeleton provides a molecular scaffold upon which signaling complexes may be assembled (Lin et al., 2001). We therefore tested whether the actin cytoskeleton may serve as a structural link between IP_3R-stores and B_2Rs. Neurons were preincubated with the cell-permeant toxin cytochalasin D, an inhibitor of actin filament polymerization. As indicated by staining with Alexa-red-labeled phalloidin, actin filaments in neurons are located mainly in the cell periphery, forming a submembrane cytoskeleton. Incubation with cytochalasin D for 20 min induced reorganization of the membrane cytoskeleton into diffuse foci near the plasma membrane. This treatment abolished activation of

hTrpC1 by BK (n = 6 of 8), whereas activation of mTrpC6 by both BK and Oxo-M remained largely unchanged (n = 4–6) (data not shown). The loss in coupling between B_2R and hTrpC1 resulted primarily from the disruption of the B_2R-IP_3R link since hTrpC1 cation currents could still be activated by cytosolic injection of $InsP_3$ (n = 3 of 3). Disruption of cytoskeletal tubulin by exposure to the microtubule inhibitor nocodozole had no effect on membrane receptor coupling to either hTrpC1 or mTrpC6 (n = 3–4, data not shown).

Tight Functional Association of B_2R to IP_3R in Perforated Microvesicles

The strong functional coupling of B_2Rs to IP_3Rs suggests that they may be associated within a tight signaling complex. We tested this by recording from perforated microvesicles excised from neural membranes (Figure 8A). First, an amphotericin-perforated patch was obtained on a neuron expressing hTrpC1, and BK was tested on the whole-cell macroscopic currents. If the cell was found responsive (e.g., Figure 8B, left panel) the patch was excised and a perforated microvesicle of ~3 μm diameter (see Experimental Procedure and Sakmann and Neher, 1995) formed in an outside-out configuration (Figures 8A and 8B). BK was then reapplied on the voltage-clamped microvesicle, and hTrpC1 currents were monitored (Figure 8B, right panel). Using this method we could observe activation of microscopic hTrpC1 currents in 6 out of 11 microvesicles tested. As shown in Figure 8B, hTrpC1 activation was reversibly blocked by local superfusion of 2APB (as well as by xestospongin C, n = 3), indicating that interaction between B_2R, PLCβ, IP_3R, and hTrpC1 was conserved in these microvesicles. In contrast, out of nine microvesicles tested with mTrpC6, none responded to BK, while six of them generated mTrpC6 inward currents in response to OAG application (data not shown). Consistent with this, only 2 out of 12 microvesicles expressing mTrpC6 (tested with subsequent application of OAG), responded to Oxo-M. This confirms the random distribution of mTrpC6 versus B_2Rs and M_1AChRs.

Coimmunoprecipitation of B_2R with IP_3R

To assess possible physical interactions between B_2R and IP_3R, we tested the ability of IP_3R_1 antibody to coimmunoprecipitate myc-tagged B_2Rs overexpressed in NG108-15 cells. As shown in Figure 8C, myc-tagged B_2Rs, but not myc-tagged M_1AChRs, were detected in IP_3R_1 immunoprecipitates, whereas both proteins were easily detected by Western blot (Figure 8D, bottom panel). In addition, IP_3R_1 antibody also coimmunoprecipitates endogenous B_2Rs but not M_1AChRs from SCG lysate (Figure 8D). Immunoprecipitates were also reprobed with antibodies against $G\alpha_{q/11}$ or $G_{oA/B}$ G protein subunits. $G\alpha_{q/11}$ subunits were most clearly part of the immunoprecipitated complex, whereas $G\alpha_{oA/B}$ subunits were not detected (data not shown).

Colocalization of IP_3R with B_2R but Not M_1AChR

Triple-label immunoconfocal microscopy was performed in sympathetic neurons maintained 3–4 days in culture to determine the cellular localization of endogenous B_2Rs and M_1AChRs versus reticular IP_3Rs. B_2R and

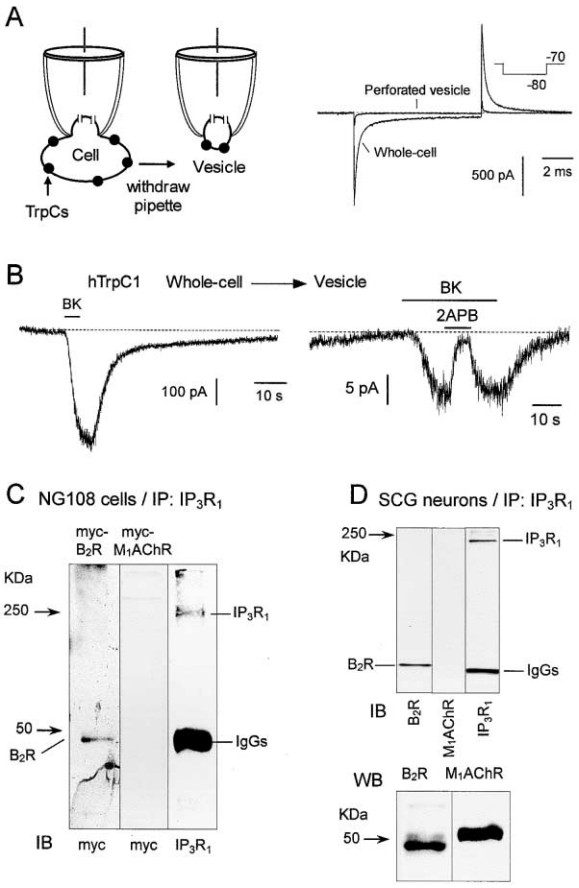

Figure 8. Docking of IP_3Rs with Plasma Membrane B_2Rs

(A and B) Same cell. (A) Schematic diagram of the manipulations performed to obtain perforated microvesicles. After cell-attached patch formation and permeabilization, the pipette was withdrawn to form an outside-out vesicle. The superimposed traces on the right show the change in membrane capacitance transients that results from the formation of the perforated vesicle. (B) hTrpC1 currents induced by BK in the whole-cell recording configuration (left panel) and in the perforated vesicle (right panel). Note the block of microscopic hTrpC1 currents by 2APB (80 μM).

(C and D) B_2R coprecipitates with IP_3R_1. (C) Detergent lysates of NG108-15 cells transfected with myc-tagged B_2R (left lane) or myc-tagged M_1AChR (middle and right) were immunoprecipitated with rabbit anti-IP_3R_1 antibody (IP) and blotted (IB) with anti-myc antibody (mouse) or rabbit anti-IP_3R_1 antibody (reprobe, right lane). Control IPs using rabbit serum or IgG fraction were negative for mouse anti-myc antibody (data not shown). Multiple high mw bands in IP_3R_1 are presumed proteolysis products. The band at ~50 kDa obtained with the anti-IP_3R_1 antibody represents reduced heavy chains of the precipitated antibody. (D) Detergent lysates of SCGs were immunoprecipitated with rabbit anti-IP_3R_1 antibody and blotted with mouse anti-B_2R, goat anti-M_1AchR, or rabbit anti-IP_3R_1 antibodies. Bottom panel, Western blot for myc-tagged B_2Rs and M_1AChRs.

M_1AChR labelings were heterogeneous in distribution, with patches of punctate labeling separated by areas in which little labeling was apparent (Figure 9A). IP_3R staining also showed punctate fluorescence within the cytoplasm and extended to the plasma membrane forming discrete patches of concentrated fluorescence, outlining the cell periphery. Simultaneous viewing of the staining patterns observed in 33 neurons revealed a close relationship between IP_3R puncta and B_2R staining

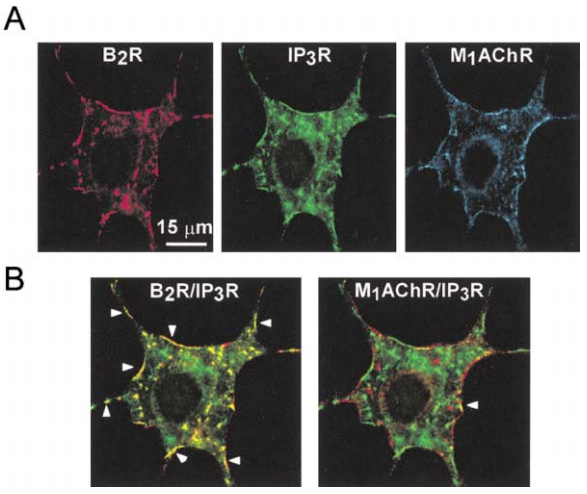

Figure 9. Colocalization of Endogenous B_2Rs with IP_3Rs

(A) Fluorescence patterns for endogenous B_2Rs, M_1AchRs, and IP_3Rs in a cultured sympathetic neuron. Cells were triple labeled with mouse monoclonal B_2R antibody (red), rabbit anti-$IP_3R_{1\text{-}3}$ polyclonal antibody (green), and goat polyclonal M_1AChR (blue). All images are reconstructions from serial optical sections.

(B) Panel showing a combined visualization of B_2R/IP_3R and M_1AChR/IP_3R labelings (Cy5-M_1AChR fluorescence was converted to red for comparison). Note that where B_2R staining occurs its distribution overlaps that of IP_3R (arrows and yellow spots).

(Figure 9B). Of 437 B_2R-positive structures, 369 (84.5%) showed juxtaposition or partial overlap with an IP_3R positive punctum. By contrast, of 511 M_1AChR-positive structures, only 89 (17.5%) were coincident or juxtaposed with IP_3R-fluorescent spots. Taken together, these data show that IP_3R-positive structures predominated adjacent to B_2R labeling and are consistent with the hypothesis that IP_3R and B_2R form functional complexes.

Discussion

The present study shows that the different Ca^{2+} signaling capabilities of B_2Rs and M_1AChRs in these (sympathetic) neurons reside in the spatio-temporal mobilization of IP_3Rs. In contrast to M_1AChRs, B_2Rs—together with $G_{q/11}$ proteins and PLCβ—are clustered with IP_3Rs to form discrete signaling complexes. These complexes enhance the efficiency of signal propagation and ensure specificity of the signaling pathway.

Transfected Trp Cation Channels as PLC Biosensors in Neurons

In our experiments, we have developed the use of Trp cation channels as sensors of PLC signaling, taking advantage of several of their unique features, including selective activation by PLC products (Harteneck et al., 2000). Perforated whole-cell recordings and immunostaining established that the homomeric hTrp1 and mTrp6 channels are expressed, inserted into the plasma membrane, and respond selectively to either DAG or $InsP_3$. Thus, by comparing the activation of hTrpC1 and mTrpC6, we could monitor the formation of $InsP_3$ and DAG in submembrane compartments, allowing real-time detection of PLC products in living neurons. Although there is good agreement that TrpC is activated downstream to PLC, the identity of the final regulatory element(s) for the multiple TrpC isoforms remains controversial. When expressed in our system, mTrpC6 was activated by DAG (or possibly one of its metabolites) in accordance with recent reports (Hofmann et al., 1999), whereas hTrpC1 was activated via the mobilization of reticular IP_3R, possibly by direct conformational coupling (Lockwich et al., 2000; Rosado and Sage, 2000; see also Boulay et al., 1999; Ma et al., 2000). In this respect, we found that myc-tagged hTrpC1 expressed in SCG neurons colocalized with native IP_3R in discrete regions of the surface membrane (our unpublished data), which makes them ideally suited for studying IP_3R signals.

This approach has clear advantages over previous methods of measuring PLC in living neurons. The most commonly used method is by monitoring inositol polyphosphate formation in large population of cells, but this affords poor spatial and temporal resolution. Other methods for tracing $InsP_3$ dynamics in single cells rely on an indirect measure with Ca^{2+}-sensing dyes (Tsien, 1998) or $InsP_3$-mediated translocation of GFP-tagged pleckstrin homology domain of PLC-δ1 (Hirose et al., 1999). Our method has the advantage in that it incorporates the PLC sensors in the surface membrane where PLC is known to reside and is therefore most suited for real-time monitoring of membrane-localized PLC signaling.

Signaling Microdomains for $InsP_3$

We have provided ample evidence that the B_2R, but not the M_1AChR, activates IP_3Rs in sympathetic neurons. Our data confirm and complement previous observations using intracellular Ca^{2+} measurements (Cruzblanca et al., 1998; del Río et al., 1999). Two arguments however demonstrate that the lack of coupling of M_1AChR to IP_3R does not result from its inability or relative inefficiency in stimulating PLCβ. First, M_1AChRs strongly activated mTrpC6 channels and translocated the DAG-sensing $C1_2$ domain of PKCγ to the plasma membrane. Second, the kinetics of M_1AChR- and B_2R-mediated production of DAG were similar. Taken together, these data indicate that both receptors are equally effective in stimulating PLC, in agreement with population-based analysis of $InsP_3$ production in SCG neurons (Bofill-Cardona et al., 2000) and with previous observations that demonstrate that both Oxo-M and BK can activate protein kinase C to open chloride channels in these cells (Marsh et al., 1995).

Instead, we suggest that the differential abilities of B_2Rs and M_1AChRs to stimulate IP_3Rs results from a more intimate relationship between the B_2Rs and the IP_3Rs. B_2Rs are not evenly distributed along the plasma membrane but instead often appear to be clustered with IP_3Rs. The endoplasmic reticulum (ER) is well known to come in close contact with the plasma membrane (Berridge, 1998; Patterson et al., 1999). Close apposition of the ER to the plasma membrane has been previously reported in rat sympathetic neurons (Henkart, 1980) where it appears to follow the contours of the somatic plasma membrane in the cell body of rat SCG neurons

(S.J. Marsh, personal communication). Clusters of B_2Rs have also been observed in neurites of differentiated neuroblastoma cells where they play a key role in initiating bradykinin-induced Ca^{2+} waves (Fink et al., 2000). The finding that the B_2R-IP_3R link was preserved in microvesicles excised from neural membrane strongly suggests that their association resembles a physical docking. This is supported by the finding that B_2R can be immunoprecipitated by IP_3R_1 antibodies. A key question therefore that arises out of these findings is how reticular IP_3Rs interact with B_2Rs. We have provided evidence that a cortical actin skeleton might play a role in stabilizing B_2R-IP_3R association, perhaps forming a bridge between the B_2R and the IP_3R by its ability to anchor both PLCβ and IP_3R. Linkage of IP_3Rs to the plasma membrane through an actin bridge has previously been reported in liver cells (Rossier et al., 1991), and Bourgignon et al. (1993) have reported that cytochalasin D also inhibits its $InsP_3$-induced Ca^{2+} release in platelets. More recently, Homer proteins have been shown to form a physical tether cross-linking mGluRs with IP_3Rs (Tu et al., 1998). Although the proline-rich Homer ligand motif is not obviously present in the B_2R, it remains to be tested whether Homer proteins or related proteins may link B_2R to IP_3R.

The fact that IP_3Rs are in close vicinity to the PLC-coupled B_2R allows them to be flooded by high $InsP_3$ concentration, which results in effective IP_3R stimulation. These signaling microdomains do not appear to have restricted $InsP_3$ diffusion, as IP_3R stimulation diminished smoothly after the stimulus had ceased; this would not be the case if $InsP_3$ was confined to specialized compartments with restricted diffusion (such as demonstrated for cAMP in HEK-293 cells; Rich et al., 2000). Thus, B_2R and M_1AChR signals do not operate in isolated subcellular compartments. As demonstrated with dominant-negative CaM, $InsP_3$ produced by the M_1AChR is not physically excluded from B_2R-IP_3R-hTrpC1 microdomains but simply does not reach a sufficient concentration with appropriate speed. One reason for this is the random distribution of M_1AChRs versus IP_3Rs. Longer and probably more intense muscarinic stimulation may therefore be required to reach $InsP_3$ levels high enough to activate IP_3Rs. It is worth noting that the level of resting cytosolic Ca^{2+} can influence M_1AChR coupling to IP_3Rs, as demonstrated by preconditioning the cell to depolarized voltages (del Río et al., 1999).

Two other important factors also contribute to attenuate Ca^{2+} signals produced by muscarinic receptor stimulation. First, the negative feedback played by CaM on IP_3R activity serves as a filter that is more efficient in inhibiting slow rather than rapid rises in $InsP_3$. Second, IP_3Rs in SCG neurons—and in neurons in general—have low affinities for $InsP_3$ in comparison with those in NG108-15 or CHO cells. These differences in sensitivities between neurons, neuroblastoma, and nonneuronal cells have been reported previously (Khodakhah and Ogden, 1993; see also Fink et al., 2000). They may explain why M_1AChRs are able to stimulate IP_3Rs in NG108-15 and CHO cells, but not in SCG neurons, and emphasize the need in neurons for high local $InsP_3$ concentrations.

A simplified view of $InsP_3$ signaling emerging from our study is depicted in Figure 10. Extracellular signals such as ACh or BK bind their respective receptors in the cell plasma membrane, which then activate the membrane-associated G proteins and PLCβ with comparable efficiencies. B_2R/PLCβ are clustered with (some) IP_3Rs, thus creating spatially compact signaling complexes. (This complex may also contain a specific isoform of PLC, PLCβ4, linked to the B_2R; see Haley et al., 2000b). This causes the Ca^{2+}-mobilizing messenger $InsP_3$ to build up in discrete domains and activate IP_3R. IP_3Rs do not form such signaling complexes with M_1AChRs, which make them "diffusionally isolated" from these receptors.

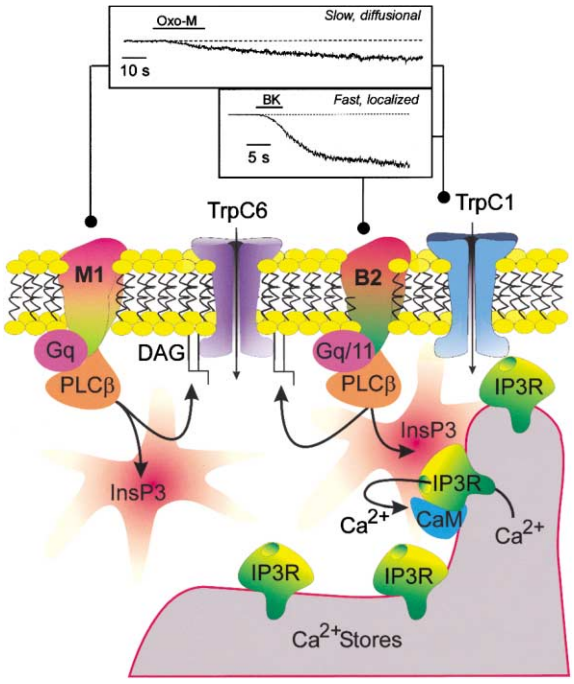

Figure 10. Model for Spatio-Temporal Coding of $InsP_3$ Signaling in SCG Neurons

Agonist activation of M_1AChRs and B_2Rs via heterotrimeric G proteins stimulates PLCβ, leading to the prodution of DAG and $InsP_3$ second messengers. Complexes of B_2Rs with reticular IP_3Rs create high local [$InsP_3$] in close proximity to the IP_3Rs, releasing Ca^{2+} from endoplasmic reticulum stores. The activation of IP_3Rs and/or the fall in luminal Ca^{2+} in the store (see Putney, 1999) induce a conformational change of the IP_3R, causing hTrpC1 to open. The signaling complexes containing B_2Rs, G proteins, PLCβ, and IP_3Rs (along with exogenous hTrpC1) requires an actin-provided scaffold to support the IP_3Rs in a position close to the plasma membrane. Although M_1AChRs activate PLCβ and consequently open mTrpC6, they fail to mobilize IP_3Rs because they are physically excluded and remote from IP_3R domains. Activation of IP_3Rs by diffusional $InsP_3$ is prevented further by the low sensitivity of IP_3R for $InsP_3$ and the inhibitory feedback played by calmodulin.

Physiological Implication of Signaling Microdomains

Localizing B_2Rs and IP_3Rs within signaling microdomains provides a mechanism for achieving specificity and efficiency by ensuring that IP_3Rs located remotely from receptors are not exposed to the same level of $InsP_3$ as those in the vicinity of the complex. This results in the coordinated gating of IP_3Rs sequestered to the

microdomain and thereby removes the need for $InsP_3$ to accumulate throughout the cytosol. This is particularly important in view of the low sensitivity of neuronal IP_3R for $InsP_3$. An example of the differential functional effects of B_2Rs and M_1AChRs in sympathetic neurons resulting from this localization concerns the mechanisms whereby they inhibit voltage-gated M channels. While activation of either receptor inhibits these channels, and thereby increases neuronal excitability (see Marrion et al., 1989; Jones et al., 1995), the mechanisms whereby they do so differ. Inhibition by B_2Rs results from the rise in Ca^{2+} produced by the tight coupling to IP_3Rs, whereas inhibition by M_1AChRs results from some other, non-PLC/Ca^{2+}-dependent mechanism (Cruzblanca et al., 1998; Haley et al., 2000a; Bofill-Cardona et al., 2000). In contrast, since both receptors stimulate the production of DAG, both activate the same PKC-dependent chloride current through a common mechanism (Marsh et al., 1995).

Nevertheless, it is clear that $InsP_3$ production is enhanced by M_1AChR stimulation in these neurons (see del Río et al., 1999, and references therein). What could be the function of this? Since the most effective stimulation of IP_3Rs is achieved when both intracellular Ca^{2+} and $InsP_3$ are presented together (Berridge, 1998), this dual activation system might act as a coincidence detector: small elevations of $InsP_3$ by M_1AChRs that are not able to cause Ca^{2+} mobilization may enhance the Ca^{2+} sensitivity of the IP_3R, thereby facilitating further PLC-mediated receptor signals.

In conclusion, the extensive and intricate network of signaling pathways requires mechanisms to achieve specificity. Here, we have described the presence of spatially restricted signaling complexes between the B_2R and the IP_3R. These signaling microdomains allow localized formation of $InsP_3$ and coordinated activation of sequestered IP_3Rs. Our data provide a framework for understanding the multiple and differential cellular functions regulated by PLC-coupled membrane receptors.

Experimental Procedures

cDNA Constructs

cDNA for hTrpC1, hTrpC3, and mTrpC6 have been kindly provided by Dr. Christian Harteneck (Institut für Pharmakologie, Freie Universität Berlin, Germany) and were subcloned into pcDNA3 or pMT vectors (Stratagene). cDNA encoding GTPase-deficient forms of $G\alpha_q$ (Q209L), $G\alpha_{11}$ (Q209L), $G\alpha_{oA}$ (Q205L), and $G\alpha_{12}$ (Q229L) were subcloned either in pcDNA1 or pcDNA3 vectors and have been described previously (Delmas et al., 1998b; Haley et al., 1998). $C1_2$ and C2 domains of PKCγ were subcloned in pEGFP-N1 vector. cDNA encoding a Ca^{2+}-insensitive mutant of calmodulin ($CaM_{1\text{-}4}$) (first D in E-F hand 1,2,3,4 mutated to A) and wt CaM were subcloned in pBK-CMV or pMT. D to A mutation in amino acids 21, 57, 94, and 130 was verified by sequencing. Mouse B_2 bradykinin receptor was in pMT. Plasmids were propagated in DH5α *Escherichia coli* and purified using maxiprep columns (Qiagen, Hilden, Germany). All plasmids were verified by sequencing.

Cell Cultures and cDNA Delivery

Sympathetic neurons were isolated from Sprague Dawley rats (2 weeks old) and cultured on glass coverslips as described previously (Delmas et al., 1998a). DNA plasmids were diluted to 100 μg/ml in Ca^{2+}-free solutions (pH 7.3) containing 0.2% FITC-dextran (70,000 MW) or rhodamine (10,000 MW) and were pressure injected into the nucleus of SCG neurons as largely described (Delmas et al., 1999; Delmas et al., 2000). Cells were maintained in culture after injection and identified for patch clamping by fluorescence microscopy. CHO hm1 and differentiated NG108-15 cells were cultured on glass coverslips in α-MEM medium supplemented with 10% fetal calf serum, 1% L-glutamine, and 1% penicilin/streptomycin. Cells were transfected 1–3 days after plating using LipofectAmine Plus (Life Technologies, Gaithersburg, MD). The plasmids of interest were cotransfected with cDNA for green fluorescent protein as marker (10:1 ratio). Recordings were made 12–24 hr after transfection.

Cytosolic Microinjection of $InsP_3$

Microinjection was made using a method similar to that used for cytoplasmic injection of antibodies (Delmas et al., 1999). Briefly, micropipettes with resistance of about 60–70 MΩ were tip filled with standard intracellular solution (300 mOsmol/l) for 1 min and back filled with the same solution containing either 1, 10, 100, or 300 μM of $InsP_3$ plus 0.2% TRITC-dextran (10 kDa). The cell of interest was first voltage clamped using the perforated patch-clamp method and then impaled with the $InsP_3$-containing micropipette. A slight negative pressure was applied to the interior of the micropipette in order to avoid leakage of $InsP_3$. Five minutes was allowed after impalement to allow the holding current to recover if any leak current developed. Cells that did not recover within 5 min were not used. The injected volume was ~0.5 pl, giving a mean dilution factor of 8, 10.4, and 4 in SCG neurons, NG108-15, and CHO cells, respectively. Final concentrations of $InsP_3$ were calculated from these dilution factors.

Translocation of GFP-Tagged PKCγ Domains

cDNA of GFP-tagged minimal $C1_2$ and C2 domains of PKCγ have been described (Oancea and Meyer, 1998). As previously shown in basophilic leukemia 2H3 cells, the C-terminal GFP tags do not affect cofactor dependence and translocation of these peptides to the plasma membrane. Experiments in SCG neurons were carried out 7–18 hr after nuclear microinjection of cDNA to obtain relatively low levels of expression. Treatment with agonists or drugs were as follows: oxotremorine-M (Oxo-M, 5 μM) for 1 min; bradykinin (BK, 500 nM) for 30 s; 1,oleoyl-2-acetyl-glycerol (OAG, 50 μM) for 5 min; and ionomycin (10 μM) for 5 min. These experiments were made in the absence of extracellular Ca^{2+} (except for ionomycin, 0.5 mM Ca^{2+}) in order to prevent Ca^{2+} influx eventually caused by drug-induced depolarization. Cells were then fixed with 4% paraformaldehyde and 0.15 M sucrose in phosphate-buffered saline (PBS) (25 min at room temperature). Images were acquired on a Zeiss Axiophot microscope or a confocal microscope and analyzed using NIH image 1.62f software.

Measurement of Intracellular Calcium

Intracellular free Ca^{2+} concentration was estimated from indo-1 fluorescence using the ratiometric method (Grynkiewicz et al., 1985). Briefly, cells were incubated with 5 mM indo-1-AM for 30–45 min and then superfused with standard bath solution for 10–20 min to allow ester hydrolysis. Indo-1 was excited at 360 nm (330–380 nm bandwidth) and the emitted light was split by a dichroic mirror to two photomultipliers (Thorn EMI QL 30) with input filter at 408 and 480 nm. The 408/480 emission ratio was digitized using a Digidata 1200 interface driven by pClamp software. Sample rate was 100 Hz. Calibration was achieved by whole-cell dialysis of SCG neurons with intracellular solutions containing known concentrations of free Ca^{2+} (Calcium Calibration Kit, adjusted for pH and osmolarity).

Patch-Clamp Recording

Whole-cell macroscopic currents were recorded using the perforated patch method as described (Haley et al., 2000a) on neurons kept 3–4 days in culture (e.g., microinjected at day 2). Briefly, amphotericin B (0.07–0.1 mg/ml in dimethylsulfoxide) was dissolved in the intracellular solution consisting of 90 mM K^+ acetate, 30 mM KCl, 3 mM $MgCl_2$, and 40 mM Hepes (adjusted to pH 7.3 with KOH, 290 mOsmol/l). When filled with this internal solution, pipette resistance was 2–3 MΩ. Access resistances after permeabilization ranged from 8–15 MΩ. The external solution consisted of 130 mM NaCl, 3 mM KCl, 1 mM $MgCl_2$, 10 mM HEPES, 0.0005 mM tetrodotoxin (TTX), 0.2–2 mM $CaCl_2$, and 11 mM glucose (adjusted to pH 7.3 with NaOH,

292 mOsmol/l). Recordings were obtained with an Axopatch 200A amplifier (Axon Instruments) and filtered at 2 kHz.

For recording of perforated microvesicles, patch pipettes were pulled from thin-walled borosilicate glass capillaries (Harvard Apparatus, UK), polished, and coated with Sylgard. They had a resistance of ~2 MΩ (1–1.25 μm tip diameter). After permeabilization (incomplete), the pipette was withdrawn from the cell to form a perforated vesicle. During this process, the patch-clamp amplifier was switched to current-clamp mode with zero resting current. Assuming an Ω-shaped geometry of these vesicles (Sakmann and Neher, 1995), the total membrane area was estimated to be 30–40 μm^2, from which the sealed membrane portion was 21 μm^2, the perforated membrane portion was 13 μm^2 and the patch area in contact with the bath was 0.8–3 μm^2.

Coimmunoprecipitation

NG108-15 cells were transfected with myc-tagged mB_2R or myc-tagged rM_1AChR cDNAs using Tfx-50 reagent. Cells were scraped in TE buffer (50 mM Tris and 1 mM EDTA, pH 7.4) containing 1% CHAPS and protease inhibitor cocktail (10 μl per 10^6 cells). Isolated SCGs were cleansed of connective tissue, cut into small pieces, and sonicated in TE buffer containing 1% CHAPS and protease inhibitor cocktail (100 mg wet weight/ml). NG108-15 and SCG homogenates were then centrifuged at 60,000–90,000 rpm at 4°C for 20 min. 1 ml of the NG108-15 cellular extract and 100 μl of SCG cellular extract were used in the immunoprecipitation assay with 1.3–3 μl anti-IP_3R_1 antibody (rabbit, Alomone labs). Antibodies and extract were then incubated for 1 hr at 4°C before adding protein G sepharose. Immunoprecipitates were washed three times in TE-CHAPS buffer, separated by SDS-PAGE, and analyzed by immunoblot. Blots of immunoprecipitated complexes were probed (or reprobed) with anti-myc antibody (mouse, 1/1000, oncogene, Research products), anti-M_1AChR antibody (goat, 1/500, Santa Cruz Biotechnology, Inc.), anti-B_2R antibody (mouse, 1/1000, Research Diagnostics, Inc), anti-IP_3R_1 antibody (rabbit, 1/1000), and anti-$G\alpha_{q/11}$ or anti-$G\alpha_{oA/B}$ antibodies (1/800, gift from Graeme Milligan) and visualized using ECL-Western blotting detection reagents (Amersham pharmacia).

Immunofluorescence

SCG neurons were fixed with 4% paraformadehyde, permeabilized with 0.1% triton, and blocked by 1% BSA (PBS buffered) for 30 min before incubation for triple labeling. The optimal procedure for triple labeling was treatment with a mixture of mouse monoclonal B_2R antibody (1/800, Research Diagnostics, Inc.) and goat polyclonal M_1AChR (1/800, Santa Cruz Biotechnology, Inc.) overnight at room temperature, followed by a rabbit polyclonal anti-$IP_3R_{1\text{-}3}$ antibody (2–4 μg/ml, Calbiochem) for 2–3 hr. Cells were washed four times and incubated with a mixture of the FITC- (sheep anti-rabbit, 1/100), Cy3- (donkey anti-mouse, 1/250), and Cy5- (donkey anti-goat, 1/250) conjugated secondary antibodies (all Chemicon, Euromedex, France) at room temperature for 1 hr. Controls involved secondary antibodies crossover experiments and competitive peptide inhibition. Images were obtained by confocal laser scanning microscopy using a Leica TCS SP equipped with krypton, argon, and helium neons lasers. Series of images were sequentially acquired to avoid signal crossover, and quantification of puncta was performed on 10 μm confocal *z*-axis stacks from 33 selected neurons.

Solutions

Solutions were made just before the experiments and applied using a gravity-fed perfusion system at 10–15 ml/min. For the experiments in Figure 3, test agents were applied to neurons through a glass micropipette (30–50 μm i.d.) placed 50 μm away from the neuron under study. Dose-response curves for Oxo-M were constructed using cumulative application of increasing concentrations of the muscarinic agonist, whereas noncumulative dose-response curves were made for BK (to avoid desensitization). Data were expressed as the mean ± SE of the mean. ANOVA and Student's t test were applied to determine the statistical significance, and differences were considered significant if $p < 0.05$. All experiments were performed at 31°C–33°C.

Acknowledgments

This study was supported by the Wellcome Trust Programme grant 038171, by a grant from the UK Medical Research Council (PG7909913), and by the CNRS. N.W. and M.M. were supported by predoctoral grants from the Department of Pharmacology, UCL. The authors wish to thank Dr. Tobias Meyer (Department of Cell Biology, Duke University, Durham, NC) for cDNA encoding $C1_2$ and C2 domains of PKCγ, Drs. Christian Harteneck and Günter Schultz (Institut für Pharmakologie, Freie Universität, Berlin, Germany) for Trp cDNAs, and Dr. Haruhiro Higashida (Department of Biophysics, University of Kanazawa, Japan) for mouse B_2R cDNA.

Received: May 30, 2001
Revised: February 6, 2002

References

Berhneim, L., Mathie, A., and Hille, B. (1992). Characterization of muscarinic receptor subtypes inhibiting Ca^{2+} current and M current in rat sympathetic neurons. Proc. Natl. Acad. Sci. USA *89*, 9544–9548.

Berridge, M.J. (1993). Cell signaling. A tale of two messengers. Nature *365*, 388–389.

Berridge, M.J. (1998). Neuronal calcium signaling. Neuron *21*, 13–26.

Bofill-Cardona, E., Vartian, N., Nanoff, C., Freissmuth, M., and Boehm, S. (2000). Two different signaling mechanisms involved in the excitation of rat sympathetic neurons by uridine nucleotides. Mol. Pharmacol. *57*, 1165–1172.

Boulay, G., Zhu, X., Peyton, M., Jiang, M., Hurst, R., Stefani, E., and Birnbaumer, L. (1997). Cloning and expression of a novel mammalian homolog of Drosophila transient receptor potential (Trp) involved in calcium entry secondary to activation of receptors coupled by the Gq class of G protein. J. Biol. Chem. *272*, 29672–29680.

Boulay, G., Brown, D.M., Qin, N., Jiang, M., Dietrich, A., Zhu, M.X., Chen, Z., Birnbaumer, M., Mikoshiba, K., and Birnbaumer, L. (1999). Modulation of Ca^{2+} entry by polypeptides of the inositol 1,4,5-triphosphate receptor (IP3R) that bind transient receptor potential (TRP): evidence for roles of TRP and IP3R in store depletion-activated Ca^{2+} entry. Proc. Natl. Acad. Sci. USA *96*, 14955–14960.

Bourgignon, L.Y., Iida, N., and Jin, H. (1993). The involvement of the cytoskeleton in regulating IP3 receptor-mediated internal Ca^{2+} release in human blood platelets. Cell Biol. Int. *17*, 751–758.

Brown, D.A., Abogadie, F.C., Allen, T.G.J., Buckley, N.J., Caulfield, M.P., Delmas, P., Haley, J.E., Lamas, J.A., and Selyanko, A.A. (1997). Muscarinic mechanisms in nerve cells. Life Sci. *60*, 1137–1144.

Caulfield, M.P. (1993). Muscarinic receptors—characterization, coupling and function. Pharmacol. Ther. *58*, 319–379.

Clapham, D.E., Runnels, L.W., and Strubing, C. (2001). The TRP ion channel family. Nat. Rev. Neurosci. *6*, 387–396.

Cruzblanca, H., Koh, D.S., and Hille, B. (1998). Bradykinin inhibits M current via phospholipase C and Ca^{2+} stores in rat sympathetic neurons. Proc. Natl. Acad. Sci. USA *95*, 7151–7156.

Delmas, P., Brown, D.A., Dayrell, M., Abogadie, F.C., Caulfield, M.P., and Buckley, N.J. (1998a). On the role of endogenous G-protein subunits in Ca^{2+} current inhibition by neurotransmitters in rat sympathetic neurones. J. Physiol. (Lond.) *506*, 319–329.

Delmas, P., Abogadie, F.C., Dayrell, M., Haley, J.E., Milligan, G., Caulfield, M.P., Brown, D.A., and Buckley, N.J. (1998b). G-proteins and G-protein subunits mediating cholinergic inhibition of N-type calcium currents in sympathetic neurons. Eur. J. Neurosci. *10*, 1654–1666.

Delmas, P., Abogadie, F.C., Milligan, G., Buckley, N.J., and Brown, D.A. (1999). βγ dimers derived from G_o and G_i proteins contribute different components of adrenergic inhibition of Ca^{2+} channels in rat sympathetic neurones. J. Physiol. (Lond.) *518*, 23–36.

Delmas, P., Abogadie, F.C., Buckley, N.J., and Brown, D.A. (2000). Calcium channel gating and modulation by transmitters depend on cellular compartmentalization. Nat. Neurosci. *3*, 670–678.

del Río, E., Bevilacqua, J.A., Marsh, S.J., Halley, P., and Caulfield,

M.P. (1999). Muscarinic M_1 receptors activate phosphoinositide turnover and Ca^{2+} mobilization in rat sympathetic neurons, but this signaling pathway does not mediate M-current inhibition. J. Physiol. (Lond.) *520*, 101–111.

Dray, A. (1997). Kinins and their receptors in hyperalgesia. Can. J. Physiol. Pharmacol. *75*, 704–712.

Dray, A., and Perkins, M. (1993). Bradykinin and inflammatory pain. Trends Neurosci. *16*, 99–104.

Fagni, L., Chavis, P., Ango, F., and Bockaert, J. (2000). Complex interactions between mGluRs, intracellular Ca^{2+} stores and ion channels in neurons. Trends Neurosci. *23*, 80–88.

Felder, C.C. (1995). Muscarinic acetylcholine receptors: signal transduction through multiple effectors. FASEB J. *9*, 619–625.

Fink, C.C., Slepchenko, B., Moraru, I.I., Watras, J., Schaff, J.C., and Loew, L.M. (2000). An image-based model of calcium waves in differentiated neuroblatoma cells. Biophys. J. *79*, 163–183.

Fukuda, K., Higashida, H., Kubo, T., Maeda, A., Akiba, I., Bujo, H., Mishina, M., and Numa, S. (1988). Selective coupling with K^+ currents of muscarinic acetylcholine receptor subtypes in NG108–15 cells. Nature *335*, 355–358.

Grynkiewicz, G., Poenie, M., and Tsien, R.Y. (1985). A new generation of Ca^{2+} indicators with greatly improved fluorescence properties. J. Biol. Chem. *260*, 3440–3450.

Hamilton, S.E., Loose, M.D., Qi, M., Levey, A.I., Hille, B., McKnight, G.S., Idzerda, R.L., and Nathanson, N.M. (1997). Disruption of the m1 receptor gene ablates muscarinic receptor-dependent M current regulation and seizure activity in mice. Proc. Natl. Acad. Sci. USA *94*, 13311–13316.

Haley, J.E., Abogadie, F.C., Delmas, P., Dayrell, M., Vallis, Y., Milligan, G., Caulfield, M.P., Brown, D.A., and Buckley, N.J. (1998). The α subunit of Gq contributes to muscarinic inhibition of the M-type potassium current in sympathetic neurons. J. Neurosci. *12*, 4521–4531.

Haley, J.E., Delmas, P., Offermanns, S., Abogadie, F.C., Simon, M.I., Buckley, N.J., and Brown, D.A. (2000a). Muscarinic inhibition of calcium current and M current in Gαq-deficient mice. J. Neurosci. *11*, 3973–3979.

Haley, J.E., Abogadie, F.C., Fernandez-Fernandez, J.M., Dayrell, M., Vallis, Y., Buckley, N.J., and Brown, D.A. (2000b). Bradykinin, but not muscarinic, inhibition of M-current in rat sympathetic ganglion neurons involves phospholipase C-β4. J. Neurosci. *20*, RC105 1–5.

Hardie, R.C., and Raghu, P. (2001). Visual transduction in *Drosophila*. Nature *413*, 186–193.

Harteneck, C., Plant, T.D., and Schultz, G. (2000). From worm to man: three subfamilies of TRP channels. Trends Neurosci. *23*, 159–166.

Henkart, M. (1980). Identification and function of intracellular calcium stores in axons and cell bodies of neurons. Fed. Proc. *39*, 2783–2789.

Hirose, K., Kadowaki, S., Tanabe, M., Takeshima, H., and Lino, M. (1999). Spatiotemporal dynamics of inositol 1,4,5-triphosphate that underlies complex Ca^{2+} mobilization patterns. Science *284*, 1527–1530.

Hofmann, T., Obukhov, A.G., Schaefer, M., Harteneck, C., Gutermann, T., and Schultz, G. (1999). Direct activation of human TRPC6 and TRPC3 channels by diacylglycerol. Nature *397*, 259–263.

Jones, S., Brown, D.A., Milligan, G., Willer, E., Buckley, N.J., and Caulfield, M.P. (1995). Bradykinin excites rat sympathetic neurons by inhibition of M current through a mechanism involving B_2 receptors and $G\alpha_{q/11}$. Neuron *14*, 399–405.

Khodakhah, K., and Ogden, D. (1993). Functional heterogeneity of calcium release by inositol triphosphate in single Purkinje neurones, cultured cerebellar astrocytes and peripheral tissues. Proc. Natl. Acad. Sci. USA *90*, 4976–4980.

Lee, S.B., and Rhee, S.G. (1995). Significance of PIP2 hydrolysis and regulation of phospholipase C isoenzymes. Curr. Opin. Cell Biol. *7*, 183–189.

Lin, R., Karpa, K., Kabbani, N., Goldman-Rakic, P., and Levenson, R. (2001). Dopamine D2 and D3 receptors are linked to the actin cytoskeleton via interaction with filamin A. Proc. Natl. Acad. Sci. USA *98*, 5258–5263.

Lockwich, T.P., Liu, X., Singh, B.B., Jadlowiec, J., Weiland, S., and Ambudkar, I.S. (2000). Assembly of Trp1 in a signaling complex associated with caveolin-scaffolding lipid raft domains. J. Biol. Chem. *275*, 11934–11942.

Ma, H.T., Patterson, R.L., van Rossum, D.B., Birnbaumer, L., Mikoshiba, K., and Gill, D.L. (2000). Requirement of the inositol triphosphate receptor for activation of store-operated Ca^{2+} channels. Science *287*, 1647–1651.

Marrion, N.V., Smart, T.G., Marsh, S.J., and Brown, D.A. (1989). Muscarinic suppression of the M-current in the rat sympathetic ganglion is mediated by receptors of the M_1- subtype. Br. J. Pharmacol. *98*, 557–573.

Marsh, S.J., Trouslard, J., Leaney, J.L., and Brown, D.A. (1995). Synergistic regulation of a neuronal chloride current by intracellular calcium and muscarinic receptor activation : a role for protein kinase C. Neuron *15*, 729–737.

Michikawa, T., Hirote, J., Kawano, S., Hiraoka, M., Yamada, M., Furuichi, T., and Mikoshiba, K. (1999). Calmodulin mediates calcium-dependent inactivation of the cerebellar type 1 inositol 1,4,5-triphosphate receptor. Neuron *23*, 799–808.

Oancea, E., and Meyer, T. (1998). Protein kinase C as a molecular machine for decoding calcium and diacylglyrerol signals. Cell *95*, 307–318.

Patterson, R.L., van Rossum, D.B., and Gill, D.L. (1999). Store-operated Ca^{2+} entry: evidence for a secretion-like coupling model. Cell *98*, 487–499.

Putney, J.W. (1999). TRP, inositol 1,4,5-trisphosphate receptors, and capacitive calcium entry. Proc. Natl. Acad. Sci. USA *96*, 14669–14671.

Rich, T.C., Fagan, K.A., Nakata, H., Schaach, J., Cooper, D.M., and Karpen, J.W. (2000). Cyclic nucleotide-gated channels colocalize with adenylyl cyclase in regions of restricted cAMP diffusion. J. Gen. Physiol. *116*, 147–161.

Robbins, J., Marsh, S.J., and Brown, D.A. (1993). On the mechanism of M-current inhibition by muscarinic m1 receptors in rodent neuroblastoma glioma cells. J. Physiol. (Lond.) *469*, 153–178.

Rosado, J.A., and Sage, S.O. (2000). Coupling between inositol 1,4,5-triphosphate receptors and human transient receptor potential channel 1 when intracellular Ca^{2+} stores are depleted. Biochem. J. *350*, 631–635.

Rossier, M.F., Bird, G.S., and Putney, J.W., Jr. (1991). Subcellular distribution of the calcium-storing inositol 1,4,5-trisphosphate-sensitive organelle in rat liver. Possible linkage to the plasma membrane through the actin microfilaments. Biochem. J. *274*, 643–650.

Sakmann, B., and Neher, E. (1995). Geometric parameters of pipettes and membrane patches. In Single-Channel Recording, B. Sakmann and E. Neher, eds. (New York: Plenum Press).

Tsien, R.Y. (1998). The green fluorescent protein. Annu. Rev. Biochem. *67*, 509–544.

Tu, J.C., Xiao, B., Yuan, J.P., Lanahan, A.A., Leoffert, K., Li, M., Linden, D.J., and Worley, P.F. (1998). Homer binds a novel proline-rich motif and links group 1 metabotropic glutamate receptors with IP3 receptors. Neuron *21*, 717–726.

Xia, X.-M., Falker, B., Rivard, A., Wayman, G., Johnson-Pais, T., Keen, J.E., Ishii, T., Hirschberg, B., Bond, C.T., Lutsenko, S., et al. (1998). Mechanism of calcium gating in small-conductance calcium-activated potassium channels. Nature *395*, 503–507.

Xiao, B., Tu, J.C., and Worley, P.-F. (2000). A link between neural activity and glutamate receptor function. Curr. Opin. Neurobiol. *10*, 370–374.

Zhu, X., Jiang, M., Peyton, M., Boulay, G., Hurst, R., Stefani, E., and Birnbaumer, L. (1996). Trp, a novel mammalian gene family essential for agonist-activated capacitative Ca^{2+} entry. Cell *85*, 661–671.